

Charge transfer in DNA*

Mamoru Fujitsuka and Tetsuro Majima[‡]

*The Institute of Scientific and Industrial Research (SANKEN), Osaka University,
Mihogaoka 8-1, Ibaraki, Osaka 567-0047, Japan*

Abstract: In the past few decades, charge transfer in DNA has attracted considerable attention from researchers in a wide variety of fields ranging from bioscience and physical chemistry to nanotechnology. Charge transfer in DNA has been investigated using various techniques. Among them, time-resolved spectroscopic methods have provided information on charge-transfer dynamics in DNA, an important basis for therapy applications, nanomaterials, and so on. In charge transfer in DNA, holes and excess electrons act as positive and negative charge carriers, respectively. Hole-transfer (HT) dynamics have been investigated in detail, while the dynamics of excess electron transfer (EET) have only become clear rather recently. In the present paper, we summarize studies on the dynamics of HT and EET by several groups including ourselves.

Keywords: charge transfer; DNA; excess electron transfer; hole transfer; hopping mechanism; laser flash photolysis; Marcus theory; nucleobases; random walk; tunneling mechanisms.

INTRODUCTION

In the past few decades, charge transfer in DNA has attracted considerable attention from researchers in a wide range of fields. Under biological conditions, DNA is constantly attacked by environmentally generated oxidants or reductants. Oxidation of DNA promotes DNA damage [1,2], while reduction of DNA is part of the repair mechanism of DNA lesions by photolyase [3–5]. Charge transfer in DNA is responsible for the remote oxidation or reduction process, i.e., the oxidation or reduction of nucleobases apart from the initially oxidized or reduced nucleobase. Electrical conductivity of DNA has also been examined for a long time because DNA exhibits a highly stacked structure of nucleobases in duplex, which is advantageous for electrical conduction [6]. Application of DNA to nanowire have been examined, and physical chemists are interested in charge transfer in DNA because of their interest in electron-transfer processes in polymeric systems, etc.

Charge transfer in DNA has been investigated using various techniques. For example, the electrical conductivity measurements showed conductivities ranging from an insulator to a superconductor [7–10]. On the other hand, product analysis of oxidative or reductive reactions of DNA has provided valuable information on charge-transfer mechanisms. Product analysis study revealed that holes and excess electrons, which are positive and negative charge carriers in DNA, respectively, can migrate rather long distances by means of a multistep hopping process [11,12]. Furthermore, investigations using time-resolved spectroscopic methods have provided information on charge-transfer dynamics in DNA including rate constants for single-step tunneling and hopping processes (Fig. 1). By using these experimental techniques, hole transfer (HT) dynamics have been investigated in detail for

Pure Appl. Chem.* **85, 1257–1513 (2013). A collection of invited papers based on presentations at the XXIVth IUPAC Symposium on Photochemistry, Coimbra, Portugal, 15–20 July 2012.

[‡]Corresponding author

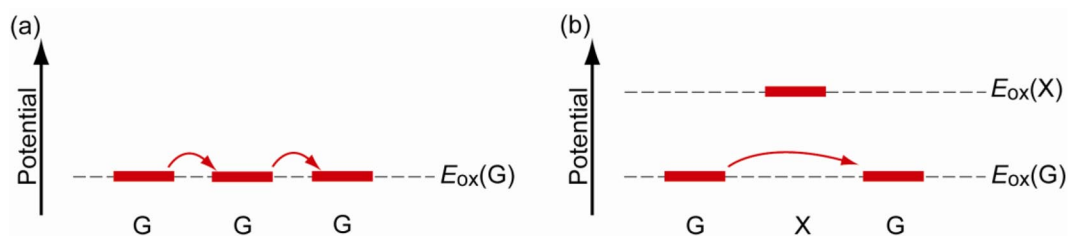


Fig. 1 Mechanisms of HT in DNA. (a) G-to-G consecutive hopping and (b) G-X-G ($X = A, C, \text{ or } T$) tunneling are indicated as representative cases. E_{ox} denotes oxidation potential.

decades, while the dynamics of excess electron transfer (EET) have become clearer more recently. Our research group has also carried out time-resolved spectroscopic studies on charge transfer in DNA [13], because the dynamics parameters provide quantitative and useful information for practical uses. In the present paper, we summarize time-resolved spectroscopic studies on HT and EET in DNA by several research groups including ourselves.

HOLE TRANSFER IN DNA

Using transient absorption spectroscopy during laser flash photolysis of DNA conjugated with a photosensitizing electron acceptor, Lewis et al. reported the distance and driving force dependencies of the hole injection processes in DNA [14–16]. From the charge separation rate between the singlet-excited stilbene dicarboxamide and G through A:T base pairs, they estimated the damping factor (β) in $k_{\text{ET}} \propto \exp(-\beta r)$ to be $\sim 0.7 \text{ \AA}^{-1}$, where k_{ET} and r are the electron-transfer rate and distance for single-step electron transfer, respectively. This value is similar to those obtained by product analysis and other time-resolved spectroscopic methods including time-resolved fluorescence measurement and pulse radiolysis [12,17]. It was shown that polyA or polyT between the photosensitizing electron acceptor and G did not cause significant difference in the β value. On the other hand, for the charge recombination process the β value was evaluated to be $\sim 0.9 \text{ \AA}^{-1}$. They attributed the larger β value of the charge recombination to its larger driving force. In addition, from the driving force dependence of the charge separation and recombination processes, they estimated 1.22 eV of reorganization energy and 347 cm^{-1} of electronic coupling when the electron acceptor and donor nucleobases were placed in the vicinity [16]. When the acceptor and donor were separated by two A:T base pairs, these values changed to 1.30 eV and 25 cm^{-1} , respectively. These values are similar to those reported for various electron-transfer systems in non-adiabatic conditions.

Our research group measured the transient absorption spectra during the laser flash photolysis of hairpin DNA consisting of A:T base pairs, which were conjugated with naphthalendiimide (NDI) and phenothiazine (PTZ) as a photosensitizing electron acceptor and donor, respectively [18]. Upon selective excitation of NDI using nanosecond laser pulse, generation of PTZ radical cation was confirmed within the laser pulse duration. Although the formation dynamics of PTZ radical cation were not observed because of the fast hole hopping among As, the distance dependence of the generation yield of PTZ radical cation (Fig. 2) indicated that PTZ radical cation was generated by multistep hopping of hole injected from the singlet-excited NDI to DNA. This is in accordance with the conclusions of product analysis works [12]. In addition, the A to A hopping rate was estimated to be $2 \times 10^{10} \text{ s}^{-1}$. Recently, Lewis and co-workers estimated the A-to-A and G-to-G hopping rates to be 1.2×10^9 and $4.3 \times 10^9 \text{ s}^{-1}$, respectively, from the direct observation of HT dynamics in photosensitizing acceptor–DNA–donor system by transient absorption spectroscopy [19]. Thus, it can be concluded that the single-step hole hopping time in As or Gs is on the order of several tens to hundreds picoseconds.

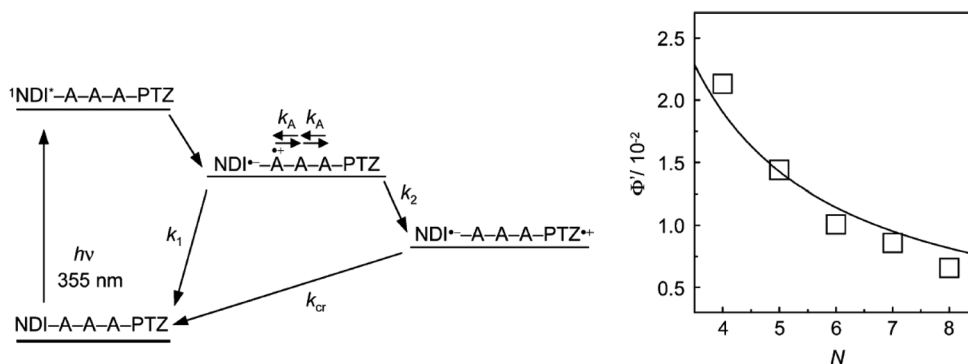


Fig. 2 (Left) Schematic diagram for the HT in NDI- and PTZ-conjugated DNA and (right) distance (N : step number) dependence of generation yield of PTZ radical cation. Reprinted with permission from *J. Am. Chem. Soc.* **126**, 1125 (2004). Copyright © (2004) American Chemical Society.

Insertion of other nucleobase(s) between As or Gs slows down the hopping rate among them, because inserted nucleobase(s) act as a barrier for the hopping (Fig. 1). We estimated hopping rates between Gs or G and C, separated by various nucleobase(s), as summarized in Table 1 [20,21]. The hopping rate depends on the type and number of nucleobase(s). These findings agree with the electron-transfer theory [22,23], that is, the electron-transfer rate depends to a large extent on the barrier height and length between the donor and acceptor. These works revealed detailed mechanisms and rate constants of HT in DNA. It should be emphasized that the rate constant of the charge-transfer process is also essential in applications such as detection of DNA sequences. For example, we showed that a single molecular fluorescence detection method can detect DNA sequences on the basis of the HT rate in DNA [24,25]. Furthermore, we found that titanium dioxide can also be used as the photosensitizing electron acceptor for the detection of the mismatch sequence [26].

Table 1 The intra- and inter-strand hole hopping rates between two Gs separated by A, T, or C and activation energy. Reprinted with permission from *Chem.—Eur. J.* **11**, 3835 (2005). Copyright © (2005) John Wiley.

Sequence	n	$k_{\text{ht}}/\text{s}^{-1}$	E_a/eV
G-A $_n$ -G	1	4.8×10^7	0.18
	2	9.7×10^4	0.43
	3	1.4×10^4	—
G-T $_n$ -G	1	4.6×10^5	0.35
	2	3.6×10^4	0.50
	3	9.1×10^3	—
G-A $_n$ -C ^a	1	1.4×10^6	0.30
	2	4.5×10^4	0.53
G-T $_n$ -C ^a	1	1.6×10^6	0.25
	2	3.1×10^4	0.50
G-C $_n$ -G ^a	1	$(3.6\text{--}4.0) \times 10^8$	0.22–0.25

^aInterstrand hole hopping rate.

EXCESS ELECTRON TRANSFER IN DNA

As summarized in the previous section, the kinetic parameters of HT in DNA have been estimated in detail. On the other hand, the dynamics of EET in DNA have not been determined. From electron spin resonance (ESR) studies on γ -ray radiated DNA, Sevilla et al. estimated the β value of single-step EET at 77 K to be 0.8–1.2 \AA^{-1} [27]. In addition, several research groups reported that the excess electron migrates in DNA by means of the multistep hopping mechanism [28–45]. Thus, the actual rate constant is necessary for further detailed understanding of EET in DNA. In the next section, we summarize the approaches for clarification of EET dynamics in DNA.

Excess electron injection to DNA

The dynamics of the excess electron injection process to DNA, i.e., photoinduced electron transfer from a photosensitizing electron donor to a nucleobase, have been investigated by means of ultrafast spectroscopic methods using a femtosecond laser as an excitation source. In 1999 and 2002, Lewis and co-workers reported the photoinduced charge separation between the singlet-excited stilbene diether and nucleobases using DNA hairpins [46,47]. In their 2002 paper, they studied the dependence on electron-accepting nucleobases and distance. They confirmed that T, C, and BrU can accept an excess electron from the singlet-excited stilbene diether. In particular, fast charge separation times within 0.5 ps were observed when T or BrU was placed next to the singlet-excited stilbene diether. In spite of similar driving forces, they found a slower excess electron injection rate for the distant donor–acceptor pair compared to that of the hole injection. They attributed the slower rate to the longer donor–acceptor distance or weaker donor–acceptor interaction resulting from a G:G base pair separating stilbene diether and the electron acceptor. On the other hand, in 2000, Zewail and his co-workers reported charge separation on the order of sub-nanoseconds between the singlet-excited aminopurine and the adjacent T or C in a DNA duplex [48]. Wagenknecht et al. reported photoinduced charge separation between singlet-excited pyrene and T or C using the dyad system [49,50]. The experiments on the pH-dependent dynamics suggested that C radical anion is protonated rapidly by surrounding water or a complementary nucleobase, G, to stabilize the excess electron. From this, they concluded that C radical anion cannot play a major role as an excess electron carrier, while T possibly acts as an excess electron carrier.

As indicated in the introduction, excess electron injection is an important process in the repair of damaged DNA by photolyase. The electron-transfer dynamics from photoexcited reduced flavin-adenine dinucleotide (FADH^-) to cyclobutane T dimer were investigated by Zhong and co-workers in 2005 [51]. They observed direct electron transfer from excited flavin cofactor to T dimer in 170 ps and back electron transfer from the repaired T in 560 ps based on the stretched exponential function. The double exponential fitting to the back electron-transfer process provided lifetimes of 0.46 and 1.24 ns. In 2011, Brettel and co-workers reported the electron-transfer and back electron-transfer rates to be 0.1 and 1.55 ns, respectively [52]. They pointed out that the time constant on the nanosecond scale can be attributed to the electron return after splitting of the dimer. Zhong and co-workers also reported the electron-transfer dynamics between FADH^- and 6-4 photoproduct of pyrimidine bases. In this case, the forward electron-transfer rate was reported to be 225 ps [53]. Therefore, in these biological systems, electron transfer in the sub-nanosecond scale seems to be dominant.

As briefly summarized above, the excess electron injection dynamics have been confirmed with various charge separation systems. However, the parameters for the electron-transfer theory, such as reorganization energy and electronic coupling [22,23] of the excess electron injection process, have not been determined. To clarify this issue, we studied the driving force dependence of the electron-transfer rate. As a photosensitizing electron donor, our research group employed oligothiophenes because of their higher electron donor ability in the singlet-excited state and clear absorption bands in the radical cation state, which are preferable in transient absorption studies. By using bithiophene (2T) as a photosensitizing electron donor against nucleobase (T, C, A, and G), free energy changes of -0.16 , -0.07 ,

0.15, and >0.46 eV were expected, respectively [54,55]. The charge separation process between the singlet-excited 2T and the nucleobase in the dyad system (Fig. 3) was examined by means of the transient absorption spectroscopy using a femtosecond laser pulse, which excited 2T selectively. In the case of **4**, in which 2T and G were connected, generation of the singlet-excited 2T followed by generation of the triplet excited state via the intersystem crossing process was confirmed. On the other hand, in the cases of **1**, **2**, and **3**, radical cation of 2T was generated with the decay of the singlet-excited 2T, indicating the photoinduced charge separation with nucleobases. This result indicates that A, a well-known hole carrier, also acts as an electron acceptor as well as T and C when the photosensitizing electron donor exhibits sufficient electron donor ability. The charge separation rates were on the order of **1** (T) $>$ **2** (C) $>$ **3** (A), which are consistent with the reduction potential of the nucleobases [56]. On the other hand, generated radical ion pairs decayed due to charge recombination generating the corresponding ground state. The rate constants of the charge recombination were on the order of **1** $>$ **2** $>$ **3**, while the driving forces for the charge recombination were **3** $>$ **2** $>$ **1**, indicating that the charge recombination process was in the Marcus inverted region. For better understanding of the present driving force dependence, the electron-transfer rates (charge separation and recombination transfer rates) were plotted against the driving force in Fig. 4. It is clear that the charge separation and charge recombination processes are in the normal and inverted regions, respectively. For the hole injection process, Lewis and co-workers reported the driving force dependence of the electron-transfer rate [16], from which they estimated the parameters for the Marcus theory [22,23], such as electronic coupling and reorganization energies. In Fig. 4, the theoretical curve based on the parameters for the hole injection process was plotted as a broken line [16]. It is clear that the electron-transfer rates of the excess electron injection process were located close to the theoretical curve for hole injection. A better fit can be obtained by employing the slightly larger internal reorganization energy and electronic coupling as shown as a solid curve in Fig. 4, indicating the similarities in the parameters in the Marcus theory. Since the data points in Fig. 4 are limited, the observed tendency is tentative, but the difference from the hole injection process is an interesting point that requires detailed analysis. In addition, determination of the damping factor (β) in $k_{\text{ET}} \propto \exp(-\beta r)$ with various sequences is an important subject that requires clarification for EET and injection processes. These studies are in progress.

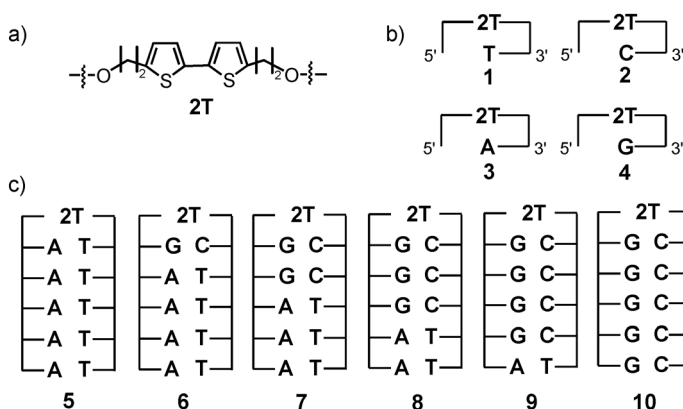


Fig. 3 Molecular structures of (a) 2T, (b) dyads **1–4**, and (c) DNA hairpins **5–10**. Reprinted with permission from *Chem.—Eur. J.* **18**, 7326 (2012). Copyright © (2012) John Wiley.

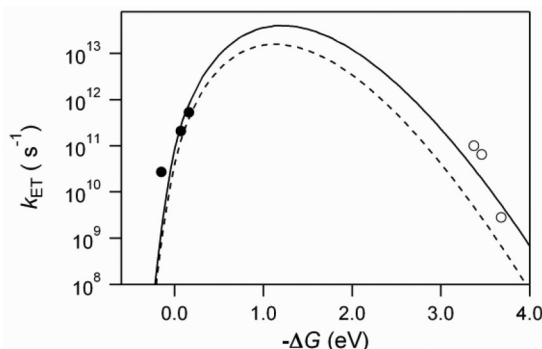


Fig. 4 ΔG (ΔG_{CS} and ΔG_{CR}) dependence of k_{ET} [k_{CS} (filled circles) and k_{CR} (open circles)]. The solid line was estimated using 0.20, 1.10, 0.070, and 0.19 eV of λ_S , λ_V , V , and $\hbar\langle\omega\rangle$, respectively. The dashed line was calculated using 0.23, 0.99, 0.043, and 0.19 eV, respectively [16]. Reprinted with permission from *Chem.—Eur. J.* **18**, 7326 (2012). Copyright © (2012) John Wiley.

EET dynamics in DNA

Product analysis studies have provided information on the excess electron hopping process. Carrel and co-workers investigated EET from excited reduced flavin to T-T dimer through A:T base pairs [28]. It is noted that their system mimics the natural photolyase system in which the EET process participates. From the cleaved yield of the T-T dimer, they confirmed a smaller distance dependence of cleaved yield, which can be expressed by 0.11 \AA^{-1} of the β value. They attributed the small distance dependence to the excess electron hopping among T. The excess electron hopping was also supported by the fact that the slope of the plot of $\log(\text{T-T dimer cleave yield})$ against $\log(\text{the number of hopping steps})$ is almost 2, indicating a 1D random walk. Rokita and Ito also demonstrated multistep excess electron hopping from product analysis of tetramethyldiaminonaphthalene- and BrU-tethered DNA [37,38]. Lewis and co-workers reported the product analysis of DNA conjugated with aminopyrene and BrU [39]. Although these research results support the excess electron hopping, the actual rate constant of the excess electron hopping has not been determined. From the product analysis studies, some expectations of the hopping rate have been reported. From the comparison with the debromination of the reduced BrU, Lewis and co-workers indicated that the single-step excess electron hopping between two BrUs separated by T is no faster than 10^7 s^{-1} [40]. Carell and co-workers reported that the electron-transfer rate along four A:T base pairs is faster than 1.8×10^7 but slower than $1.4 \times 10^8 \text{ s}^{-1}$, from the comparison with the T-T bond cleavage rate and debromination rate of reduced BrU [35].

To directly estimate the excess electron hopping rate in DNA, a time-resolved study using a photosensitizing electron donor–DNA–acceptor system is essential. For this purpose, we investigated the nicked dumbbell DNA conjugated with tetrathiophene (4T) and diphenylacetylene (DPA) as the photosensitizing electron donor and acceptor, respectively (Fig. 5) [57]. It was shown that the singlet-excited 4T can selectively reduce T, while the reduction potential of DPA is sufficient to accept an electron from the reduced T (Fig. 5c). For this study, we prepared the conjugated DNAs, in which 4T and DPA were separated by A:T base pairs (Fig. 5b). The transient absorption spectra during the femtosecond laser flash photolysis indicated the excess electron injection from the singlet-excited 4T to T within 10 ps (Fig. 6a). The generation of DPA radical anion with a 100 ps rise time constant (Fig. 6b) indicates a reduction of DPA by the excess electron injected into the DNA. The indicated mechanism is also supported by the distance dependence of the rise rate of DPA radical anion. The T-to-T excess electron hopping rate was determined to be $4.4 \times 10^{10} \text{ s}^{-1}$, based on the 1D random walk model [19]. It was shown that the estimated rate constant is similar to or faster than that of the A-to-A or G-to-G hole-hopping rate [18,19].

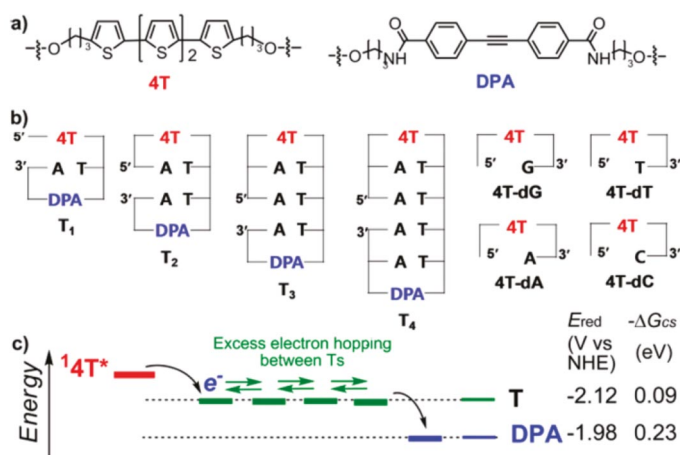


Fig. 5 (a) Molecular structures of tetrathiophene derivative (4T) and DPA conjugated to DNA. (b) Structures of nicked dumbbell DNA conjugated with 4T and DPA. (c) Simplified illustration of EET mechanism in the present DNA systems. The reduction potentials (E_{red}) of thymine and DPA and driving force for the generation of each charge separated states (ΔG_{CS}) are also indicated. Reprinted with permission from *J. Am. Chem. Soc.* **133**, 15320 (2011). Copyright © (2011) American Chemical Society.

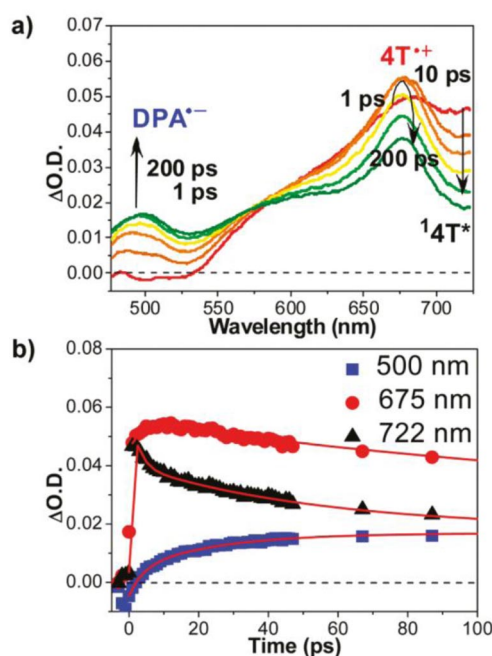


Fig. 6 Transient absorption spectra and the kinetic traces during the laser flash photolysis of T₃ upon excitation with 400-nm femtosecond laser pulse. (a) Transient absorption spectra of T₃ at 1, 10, 20, 50, 100, and 200 ps after excitation. (b) The kinetic traces of T₃ at 500 (square), 675 (circle), and 722 nm (triangle). Reprinted with permission from *J. Am. Chem. Soc.* **133**, 15320 (2011). Copyright © (2011) American Chemical Society.

EET processes in T consecutive sequences were also investigated by using DNA hairpins conjugated with *N,N*-dimethylaminopyrene (APy) and DPA as a photosensitizing electron donor and acceptor, respectively (Fig. 7) [58], because DPA is reported to form a stable hairpin structure [59,60]. Circular dichroism spectra and melting temperatures revealed that **4**, **5**, and **6** formed stable double helix structures. Transient absorption spectra during the femtosecond laser flash photolysis of **4** indicated initial generation of APy radical cation followed by the generation of DPA radical anion as evident in the normalized spectra (inset of Fig. 8a), indicating EET in consecutive T sequence. The generation kinetics of DPA radical anion were obtained as shown in Fig. 8b. It is noted that the generation

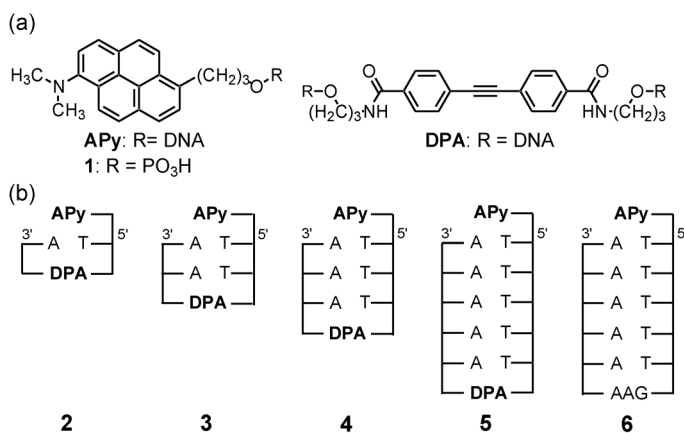


Fig. 7 (a) Molecular structures of APy and DPA. (b) Structures of DNA hairpins conjugated with APy and DPA. Reprinted with permission from *Chem. Commun.* **48**, 11008 (2012). Copyright © (2012) Royal Society of Chemistry.

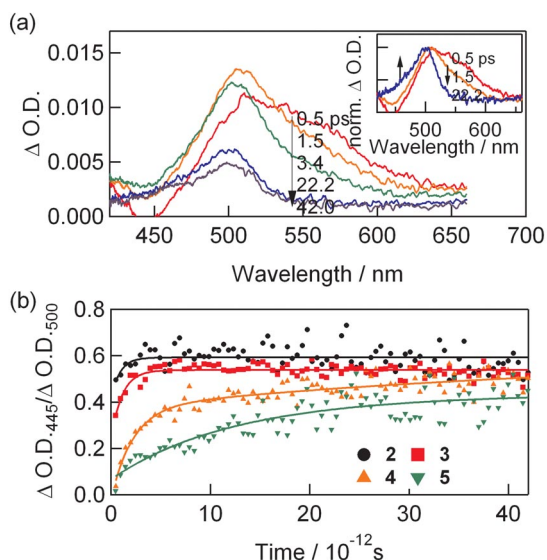


Fig. 8 (a) Transient absorption spectra of **4** in Fig. 7 during the laser flash photolysis using a 360-nm femtosecond laser pulse. Inset: Normalized spectra at 0.5, 1.5, and 22.2 ps. (b) Time dependence of ratio of ΔO.D. at 445 nm to that of 500 nm. The solid lines are the fitted curves. Reprinted with permission from *Chem. Commun.* **48**, 11008 (2012). Copyright © (2012) Royal Society of Chemistry.

dynamics of DPA radical anion in **2** and **3** were almost the same, which can be explained by assuming that APy is intercalated to the terminal nucleobases as indicated by Lewis et al. [61]. By assuming the intercalation for **4** and **5**, the single-step hopping rate of the excess electron among Ts was estimated to be $6.1 \times 10^{10} \text{ s}^{-1}$. The obtained rate is slightly faster than that estimated from the nicked dumbbell DNA conjugated with 4T and DPA, probably due to the hairpin structure and/or intercalation of a photosensitizing electron donor to the terminal base pairs. Furthermore, the present result confirms a faster EET among Ts than HT among As or Gs.

At the present stage of our study, excess electron hopping rates in other DNA sequences have not been determined. On the other hand, we found that the two block DNA hairpins, which include A:T and G:C base pairs as well as 2T, exhibited a long-lived charge-separated state indicative of C-to-C hopping on the order of 10^9 – 10^{10} s^{-1} (**5–10** in Fig. 3) [54,55]. Determination of an accurate rate constant is in progress, and DNA structure dependence of the hopping rate is another important subject to be clarified.

Sequence dependence of EET in DNA

The sequence dependence of EET in DNA has also been investigated by means of product analysis by several researchers. In 2004, Ito and Rokita reported the sequence dependence of the debromination yield of BrU as a consequence of EET in DNA. From the comparison of the yield, they provided the following conclusions [38]: (1) Contribution of C in EET is limited by preferential protonation of C radical anion over T radical anion. (2) EET from 3' to 5' direction occurs favorably than that from 5' to 3'. This tendency is opposite to that reported for HT. The effects of C in EET are also pointed out by other research groups [34,41].

Our research group measured the transient absorption spectra of donor–DNA–acceptor systems, in which *N*-methyl-*N*-pyrenylglycine (^APy) and DPA acted as a photosensitizing donor and acceptor, respectively [62]. In these systems, EET in DNA finished within the instrumental limitation (<10 ns), thus, the initial absorbance of DPA radical anion should be proportional to the yield of EET in DNA. In this study, we inserted dihydrothymine (^DT) between the electron donor and nucleobases in order to enhance the excess electron injection yield, because ^DT can act as a spacer or barrier for the initial charge recombination process between donor radical cation and nucleobase radical anion. Enhancement of excess electron injection by insertion of ^DT was confirmed. From the investigations on several DNAs, the following tendencies were confirmed. Small EET yields were observed from DNAs with the T:C and T:T mismatches indicating retardation of EET, while more stable T:G mismatch made EET possible to some extent. Replacement of A:T pairs by G:C also decreased the EET yield, although the yield is similar to that of the consecutive G:C sequence, indicating that C is not as severe EET trap as G is in HT. On the other hand, replacement of A:T by C:G decreased the yield due to the slower T-G-T hopping, in which G acts as a barrier for EET. The observed tendencies in sequence dependence of EET seem reasonable on the basis of the results reported by other research groups using product analysis. These tendencies will be discussed more quantitatively based on the actual rate constants, which will be measured in the near future.

CONCLUSION

The present paper summarized charge-transfer dynamics in DNA. Time-resolved spectroscopic studies revealed various aspects of HT dynamics including the rate constants for single-step hole injection and hopping processes. Both processes are well characterized on the basis of the Marcus theory. Furthermore, detailed information such as sequence dependence and DNA structure dependence provides a basis for future applications in fields such as therapy and nanomaterials. On the other hand, our understanding of EET is still limited. In particular, due to limited study, the dynamics of EET are still not clear. The faster EET rate than the HT rate is fascinating from the viewpoints of mechanistic study and applications. To these ends, detailed studies on the dynamics, including sequence and

structure dependence, are required. We believe that the dynamics of EET in DNA will become clear in the near future.

ACKNOWLEDGMENTS

We are grateful to a number of collaborators, especially Prof. Kiyohiko Kawai, Prof. Takashi Tachikawa, and Dr. Man Jae Park, SANKEN, Osaka University. This work has been partly supported by a Grant-in-Aid for Scientific Research (Project 22245022 and others) from the Ministry of Education, Culture, Sports, Science and Technology (MEXT) of Japanese Government. T.M. thanks the WCU (World Class University) program funded by the Ministry of Education, Science and Technology through the National Research Foundation of Korea (R31-2008-10035-0) for the support.

REFERENCES

1. C. J. Burrows, J. G. Muller. *Chem. Rev.* **98**, 1109 (1998).
2. B. Armitage. *Chem. Rev.* **98**, 1171 (1998).
3. T. Carell. *Angew. Chem., Int. Ed. Engl.* **34**, 2491 (1995).
4. A. Sancar. *Biochemistry* **33**, 2 (1994).
5. J. S. Taylor. *Acc. Chem. Res.* **27**, 76 (1994).
6. D. D. Eley, D. I. Spivey. *Trans. Faraday Soc.* **58**, 411 (1962).
7. H.-W. Fink, C. Schonberger. *Nature* **398**, 407 (1999).
8. D. Porath, A. Bezryadin, S. de Vries, C. Dekker. *Nature* **403**, 635 (2000).
9. S. Priyadarshy, S. M. Risser, D. N. Beratan. *J. Phys. Chem.* **100**, 17678 (1996).
10. M. Taniguchi, T. Kawai. *Physica E* **33**, 1 (2006).
11. B. Giese. *Acc. Chem. Res.* **33**, 631 (2000).
12. B. Giese, J. Amaudrut, A.-K. Kohler, M. Spormann, S. Wessely. *Nature* **412**, 318 (2001).
13. M. Fujitsuka, T. Majima. *Phys. Chem. Chem. Phys.* **14**, 11234 (2012).
14. F. D. Lewis, T. Wu, Y. Zhang, R. L. Letsinger, S. R. Greenfield, M. R. Wasielewski. *Science* **277**, 673 (1997).
15. F. D. Lewis, T. Wu, X. Liu, L. Letsinger, S. R. Greenfield, S. E. Miller, M. R. Wasielewski. *J. Am. Chem. Soc.* **122**, 2889 (2000).
16. F. D. Lewis, R. S. Kalgutkar, Y. Wu, X. Liu, J. Liu, R. T. Hayes, S. E. Miller, M. R. Wasielewski. *J. Am. Chem. Soc.* **122**, 12346 (2000).
17. K. Kawai, T. Takada, S. Tojo, N. Ichinose, T. Majima. *J. Am. Chem. Soc.* **123**, 12688 (2001).
18. T. Takada, K. Kawai, X. Cai, A. Sugimoto, M. Fujitsuka, T. Majima. *J. Am. Chem. Soc.* **126**, 1125 (2004).
19. S. M. M. Conron, A. K. Thazhathveetil, M. R. Wasielewski, A. L. Burin, F. D. Lewis. *J. Am. Chem. Soc.* **132**, 14388 (2010).
20. T. Takada, K. Kawai, M. Fujitsuka, T. Majima. *Chem.—Eur. J.* **11**, 3835 (2005).
21. Y. Osakada, K. Kawai, M. Fujitsuka, T. Majima. *Proc. Natl. Acad. Sci. USA* **103**, 18072 (2006).
22. R. A. Marcus. *Annu. Rev. Phys. Chem.* **15**, 144 (1964).
23. R. A. Marcus, N. Sutin. *Biochim. Biophys. Acta* **811**, 265 (1985).
24. T. Takada, M. Fujitsuka, T. Majima. *Proc. Natl. Acad. Sci. USA* **104**, 11179 (2007).
25. T. Takada, Y. Takeda, M. Fujitsuka, T. Majima. *J. Am. Chem. Soc.* **131**, 6656 (2009).
26. T. Tachikawa, Y. Asanoi, K. Kawai, S. Tojo, A. Sugimoto, M. Fujitsuka, T. Majima. *Chem.—Eur. J.* **14**, 1492 (2008).
27. A. Messer, K. Carpenter, K. Forzley, J. Buchanan, S. Yang, Y. Razskazovskii, Z. Cai, M. D. Sevilla. *J. Phys. Chem. B* **104**, 1128 (2000).
28. C. Behrens, L. T. Burgdorf, A. Schwogler, T. Carell. *Angew. Chem., Int. Ed.* **41**, 1763 (2002).
29. C. Behrens, M. Ober, T. Carell. *Eur. J. Org. Chem.* 3281 (2002).

30. C. Behrens, T. Carell. *Chem. Commun.* 1632 (2003).
31. S. Breeger, U. Hennecke, T. Carell. *J. Am. Chem. Soc.* **126**, 1302 (2004).
32. M. K. Cichon, C. H. Haas, F. Grolle, A. Mees, T. Carell. *J. Am. Chem. Soc.* **124**, 13984 (2002).
33. C. Haas, K. Kraeling, M. Cichon, N. Rahe, T. Carell. *Angew. Chem., Int. Ed.* **43**, 1842 (2004).
34. A. Manetto, S. Breeger, C. Chatgililoglu, T. Carell. *Angew. Chem., Int. Ed.* **45**, 318 (2006).
35. D. Fazio, C. Trindler, K. Heil, C. Chatgililoglu, T. Carell. *Chem.—Eur. J.* **17**, 206 (2011).
36. S. Breeger, M. von Meltzer, U. Hennecke, T. Carell. *Chem.—Eur. J.* **12**, 6469 (2006).
37. T. Ito, S. E. Rokita. *J. Am. Chem. Soc.* **125**, 11480 (2003).
38. T. Ito, S. E. Rokita. *Angew. Chem., Int. Ed.* **43**, 1839 (2004).
39. P. Daublain, A. K. Thazhathveetil, Q. Wang, A. Trifonov, T. Fiebig, F. D. Lewis. *J. Am. Chem. Soc.* **131**, 16790 (2009).
40. P. Daublain, A. K. Thazhathveetil, V. Shafirovich, Q. Wang, A. Trifonov, T. Fiebig, F. D. Lewis. *J. Phys. Chem. B* **114**, 14265 (2010).
41. C. Wagner, H.-A. Wagenknecht. *Chem.—Eur. J.* **11**, 1871 (2005).
42. L. Valis, Q. Wang, M. Raytchev, I. Buchvarov, H.-A. Wagenknecht, T. Fiebig. *Proc. Natl. Acad. Sci. USA* **103**, 10192 (2006).
43. U. Wenge, J. Wengel, H.-A. Wagenknecht. *Angew. Chem., Int. Ed.* **51**, 10026 (2012).
44. B. Elias, F. Shao, J. K. Barton. *J. Am. Chem. Soc.* **130**, 1152 (2008).
45. K. Maie, K. Miyogi, T. Takada, M. Nakamura, K. Yamana. *J. Am. Chem. Soc.* **131**, 13188 (2009).
46. F. D. Lewis, X. Liu, Y. Wu, S. E. Miller, M. R. Wasielewski, R. L. Letsinger, R. Sanishvili, A. Joachimiak, V. Tereshko, M. Egli. *J. Am. Chem. Soc.* **121**, 9905 (1999).
47. F. D. Lewis, X. Liu, S. E. Miller, R. T. Hayes, M. R. Wasielewski. *J. Am. Chem. Soc.* **124**, 11280 (2002).
48. C. Wan, T. Fiebig, O. Schiemann, J. K. Barton, A. H. Zewail. *Proc. Natl. Acad. Sci. USA* **97**, 14052 (2000).
49. N. Amann, E. Pandurski, T. Fiebig, H.-A. Wagenknecht. *Chem.—Eur. J.* **8**, 4877 (2002).
50. M. Raytchev, E. Mayer, N. Amann, H.-A. Wagenknecht, T. Fiebig. *ChemPhysChem* **5**, 706 (2004).
51. Y.-T. Kao, C. Saxena, L. Wang, A. Sancar, D. Zhong. *Proc. Natl. Acad. Sci. USA* **102**, 16128 (2005).
52. V. Thiagarajan, M. Byrdin, A. P. M. Eker, P. Müller, K. Brettel. *Proc. Natl. Acad. Sci. USA* **108**, 9042 (2011).
53. J. Li, Z. Liu, C. Tan, X. Guo, L. Wang, A. Sancar, D. Zhong. *Nature* **466**, 887 (2010).
54. M. J. Park, M. Fujitsuka, K. Kawai, T. Majima. *Chem.—Eur. J.* **18**, 2056 (2012).
55. M. J. Park, M. Fujitsuka, K. Kawai, T. Majima. *Chem.—Eur. J.* **18**, 7326 (2012).
56. C. A. M. Seidel, A. Schulz, M. H. M. Sauer. *J. Phys. Chem.* **100**, 5541 (1996).
57. M. J. Park, M. Fujitsuka, K. Kawai, T. Majima. *J. Am. Chem. Soc.* **133**, 15320 (2011).
58. M. J. Park, M. Fujitsuka, H. Nishitera, K. Kawai, T. Majima. *Chem. Commun.* **48**, 11008 (2012).
59. F. D. Lewis, X. Liu, S. E. Miller, R. T. Hayes, M. R. Wasielewski. *J. Am. Chem. Soc.* **124**, 14020 (2002).
60. T. Takada, K. Kawai, M. Fujitsuka, T. Majima. *Angew. Chem., Int. Ed.* **45**, 120 (2006).
61. K. Siegmund, P. Daublain, Q. Wang, A. Trifonov, T. Fiebig, F. D. Lewis. *J. Phys. Chem. B* **113**, 16276 (2009).
62. K. Tainaka, M. Fujitsuka, T. Takada, K. Kawai, T. Majima. *J. Phys. Chem. B* **114**, 14657 (2010).